Spin-polarized positron annihilation measurements of polycrystalline Fe, Co, Ni, and Gd based on Doppler broadening of annihilation radiation

Atsuo Kawasuso,[*] Masaki Maekawa, Yuki Fukaya, Atsushi Yabuuchi, and Izumi Mochizuki

Advanced Science Research Center, Japan Atomic Energy Agency, 1233 Watanuki, Takasaki, Gunma 370-1292, Japan

The Doppler broadening of annihilation radiation (DBAR) spectra of Fe, Co, Ni, and Gd polycrystals measured using spin-polarized positrons from a ^{68}Ge-^{68}Ga source in magnetic fields exhibited clear asymmetry upon field reversal. The differential DBAR spectra between field-up and field-down conditions were qualitatively reproduced in calculations considering polarization of positrons and electrons. The magnitudes of the field-reversal asymmetry for the Fe, Co, and Ni samples was approximately proportional to the effective magnetization. The magnetic field dependence of the DBAR spectrum for the Fe sample showed hysteresis that is similar to a magnetization curve. These results demonstrate that spin-polarized positron annihilation spectroscopy will be useful in studying magnetic substances.

The electron momentum distribution of a magnetic substance observed using spin-polarized positrons exhibits so-called field-reversal asymmetry due to the time-reversal symmetry breaking arising from excess electron spins.[1] This spectroscopic feature is analogous to that of the magnetic Compton scattering performed with circularly polarized x rays. One advantage of spin-polarized positron annihilation spectroscopy (SP-PAS) may be the depth selectivity by employing monochromatic positron beams.[2–4] Some important magnetic effects, such as giant magnetoresistance and tunneling magnetoresistance, occur near the interface between magnetic and nonmagnetic layers. Spin-injection electrodes, which will be used in spin devices, are normally thin films. Spin phenomena such as the spin Hall effect[5] and the giant Rashba effect[6] occur near surfaces. These are potential applications of SP-PAS. A pioneering research on surface magnetism using spin-polarized positron beam was performed by the Michigan group.[7] Taking advantage of the fact that PAS is a powerful tool to detect vacancy defects, SP-PAS might be used in studying vacancy-induced magnetism. In the 1960s, extensive studies were performed on magnetic substances using the angular correlation of annihilation radiation (ACAR) method with spin-polarized positrons.[8–18] However, thereafter, only a limited number of works have been carried out.[19–24]

The detection limit of the field-reversal asymmetry of the electron momentum distribution in the SP-PAS experiment depends on positron polarization. To perform better SP-PAS experiments, highly spin-polarized positrons are needed. Positrons emitted from radioisotopes are longitudinally spin polarized due to the parity nonconservation in the weak interaction.[25,26] The longitudinal spin polarization of a positron is given as its helicity, v/c, where v and c are positron and light speeds, respectively. This means that highly spin-polarized positrons can be obtained from radioisotopes with high Q values. The average helicities of positrons from ^{22}Na and ^{68}Ge-^{68}Ga are 0.7 and 0.94, respectively, and hence the latter radioisotope may be a better choice. Having positrons emitted into a cone angle θ, the average longitudinal spin polarization is decreased by a factor of $(1 + \cos\theta)/2$. Selection of faster positrons and restriction of the cone angle are options for enhancing spin polarization.[27]

In this study, for future applications of SP-PAS to spin-electronics materials, we produced a ^{68}Ge-^{68}Ga source and conducted Doppler broadening of annihilation radiation (DBAR) measurements for simple ferromagnetic substances (Fe, Co, Ni, and Gd). We considered the observed field-reversal asymmetry of DBAR spectra based on first-principles calculations.

Samples used in this study were polycrystalline Fe(4N), Co(5N), Ni(5N), and Gd(3N) with the dimension of $15 \times 15 \times 2$ mm^3. The samples were mechanically and electrochemically polished and subjected to heat treatment at 1150 °C for 2 h in vacuum. Through a nuclear reaction of ^{69}Ga$(p,2n)^{68}$Ge induced by 20 MeV proton irradiation of a GaN substrate (8 mm ϕ), a positron source (^{68}Ge-^{68}Ga, 20 MBq) was produced (total fluence: 9×10^{17} protons). In the present experimental condition, the longitudinal spin polarization of positrons emitted from the source was determined to be 0.7 through the magnetic field dependence of the S parameter related to the self-annihilation of spin-singlet positronium in α-SiO$_2$.[28] The samples and the source were placed in the center of the gap of an electromagnet keeping a distance of 7 mm at room temperature. To detect annihilation radiation only from the samples, the source was shielded by lead blocks. The DBAR spectra were measured using a high-purity Ge detector with an energy resolution of 1.4 keV at 511 keV. Here, a photon energy of $E_\gamma = 1$ keV corresponds to an electron momentum of $p = 3.92 \times 10^{-3} m_0 c$. By changing field polarity, the DBAR spectra [$N_\uparrow(p)$ and $N_\downarrow(p)$] were obtained for each sample. The subscript ↑ or ↓ denotes that the positron polarization and the magnetic field directions were parallel (field-up) or antiparallel (field-down). In each spectrum, more than 5×10^6 events were accumulated. All the spectrum area intensities were normalized to unity.

Figure 1 shows the DBAR spectra of the Fe sample obtained in the field-up and field-down conditions. It is seen that the spectrum in the field-up condition is broader than that in the field-down condition. Similar features were observed for the other samples. Figure 2 shows the differential DBAR spectra [$N_\uparrow(p) - N_\downarrow(p)$] for these samples. The finite differential intensities mean that there exists field-reversal asymmetry. Roughly speaking, the field-reversal asymmetry appears due
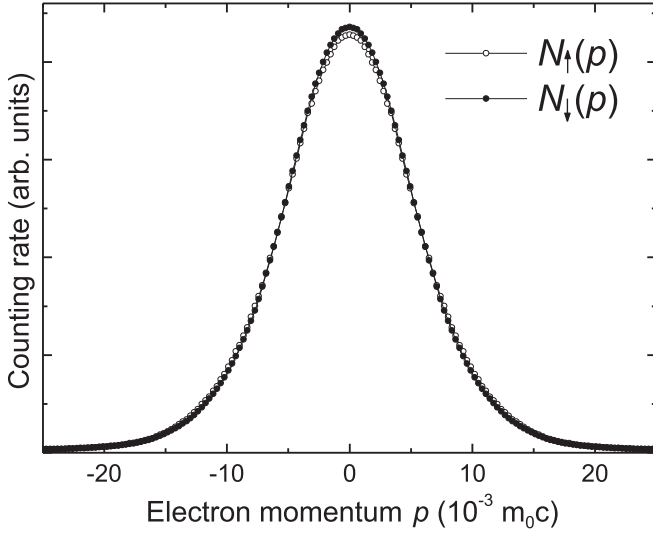
FIG. 1. DBAR spectra of the Fe sample obtained in the field-up ($\uparrow$) and the field-down ($\downarrow$) conditions at room temperature. The area intensities are normalized to unity. The errors of individual data points are within the circles.

to enhanced annihilation between spin-up positrons and spin-down $3d$ (Fe, Co, and Ni) and $4f$ (Gd) unpaired electrons. The field-reversal asymmetry of the Fe sample is the strongest, while it is slightly weaker for the Co sample, and only a small effect is observed for the Ni and Gd samples.

To interpret the above field-reversal asymmetry of the DBAR spectra theoretically, we follow Berko's method.[12] The DBAR spectrum of a magnetic substance under the field-up (field-down) condition is given by

$$N_{\uparrow(\downarrow)}(p) = \frac{\lambda_S}{8\lambda_+}(1 \pm P) \sum_{i=1}^{\text{occ.}}(1 - E_i)n_i N_i(p)$$
$$+ \frac{\lambda_S}{8\lambda_-}(1 \mp P) \sum_{i=1}^{\text{occ.}}(1 + E_i)n_i N_i(p), \quad (1)$$

where $\lambda_S = 4\pi r_e^2 c$ (r_e: the classical electron radius), P is the longitudinal polarization of positrons, and n_i, E_i, and $N_i(p)$ are the occupancy ($\leqslant 1$), the polarization, and the DBAR spectrum, respectively, of the ith band; $\lambda_{+(-)}$ is given by

$$\lambda_{+(-)} = \frac{1}{4} \sum_{i=1}^{\text{occ.}}[\lambda_S(1 \mp E_i) + \lambda_T(3 \pm E_i)]n_i w_i. \quad (2)$$

Here, $\lambda_T = \lambda_S/1115$ and w_i is the overlap integral between the positron and ith-band wave functions [$= \int_{-\infty}^{+\infty} N_i(p)dp$]. Explicitly, $\lambda_{+(-)}$ denotes the total annihilation rate of spin-up (spin-down) positrons. This means that the spin-averaged positron lifetime will be split into two components. The summation goes over all the occupied states. $N_i(p)$ is calculated from the convolution of the apparatus resolution function and the double integral of electron-positron momentum density of the ith band that is given by

$$\rho_i(\mathbf{p}) = \left| \int e^{-i\mathbf{p}\mathbf{r}} \Psi_+(\mathbf{r})\Psi_i(\mathbf{r})\sqrt{\gamma[n_-(\mathbf{r})]}d\mathbf{r} \right|^2, \quad (3)$$

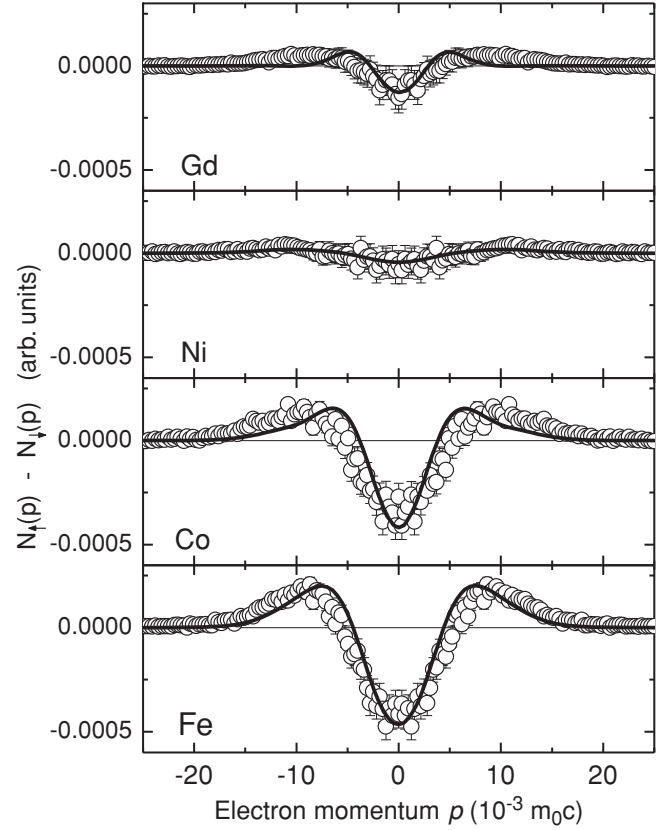where $\gamma[n_-(\mathbf{r})]$ is the enhancement factor.[29]

FIG. 2. Differential DBAR spectra $[N_{\uparrow}(p) - N_{\downarrow}(p)]$ of the Fe, Co, Ni, and Gd samples obtained in the external magnetic field of 1 T at room temperature. These spectra are folded at $p = 0$ to enhance the statistics. Solid lines denote calculated differential DBAR spectra. The amplitudes are adjusted to levels comparable with the experiments.

In this study, the electron wave functions [$\Psi_i(\mathbf{r})$] were calculated together with n_i and E_i using the ABINIT code.[30] The positron wave function [$\Psi_+(\mathbf{r})$] was calculated based on two-component density functional theory. The resolution function was assumed to be a Gaussian distribution. The details of calculations are described elsewhere.[31] The initial valence electron configurations were $3s^2 3p^6 3d^6 4s^2$ (Fe), $3s^2 3p^6 3d^7 4s^2$ (Co), $3s^2 3p^6 3d^8 4s^2$ (Ni), and $4f^7 5s^2 5p^6 5d^1 6s^2$ (Gd). The spin-averaged annihilation rates were assumed to be 9 ns^{-1} (Fe, Ni, and Co) and 4.1 ns^{-1} (Gd). Having the calculated E_i, n_i, and w_i, the $\lambda_{+(-)}$ values were 9.7 (8.3) ns^{-1} for Fe, 9.8 (8.2) ns^{-1} for Co, 9.2 (8.8) ns^{-1} for Ni, and 6.1 (2.1) ns^{-1} for Gd. Since the present samples were polycrystals, the DBAR spectra along three-momentum axes ([100], [110], and [111] for Fe and Ni, and [1100], [1120], and [0001] for Co and Gd) were spherically averaged.[19] Theoretical differential DBAR spectra were obtained as shown by solid lines in Fig. 2. The amplitudes are adjusted to a comparable level as for the experiments. The experimental differential DBAR spectra are qualitatively explained by the above calculation.

The field-reversal asymmetry of the DBAR spectrum appears due to the change of annihilation rates between polarized electrons and positrons upon field reversal. Under the field-up condition, polarized positrons tend to two-photon annihilate with polarized electrons in the spin-singlet state,

while under the field-down condition this annihilation mode is greatly reduced because the annhilation rate from the spin-triplet state is sufficiently low. Consequently, positrons tend to annihilate with the remaining electrons and the DBAR spectrum is modulated upon field reversal. In the case of Fe, Co, and Ni, $3d$ electrons that have broader momentum distributions than those of $4s$ electrons are responsible for such a polarization effect. The hybridized sd bands might also result in the sharp dip around $p = 0$ due to the negative polarizations.[9,32,33] In the case of Gd, $4f$ electrons are mainly responsible for the field-reversal asymmetry.

The field-reversal asymmetry of the DBAR spectrum may be related to the Fermi-surface (FS) topology. For instance, in Fe, the sizes of N-centered hole pockets of the third minority band and the Γ-centered FS of the sixth majority band play important roles in the field-reversal asymmetry of the ACAR spectrum.[22,32,33] The present band calculation supports such claims. However, because of the poor momentum resolution of the DBAR method and polycrystal samples used in this study, a further discussion in terms of FS is not given here.

In the differential ACAR spectra of Fe and Ni single crystals upon field reversal, some fine structures were observed around $p = 0$.[9,10,13,15–18,22,23] However, different authors reported different crystal orientations for such fine structures. For Co and Gd, no distinct fine structures were observed.[13,14,24] Contrarily, the magnetic Compton profies of Fe, Ni, and Co single crystals exhibit clear anisotropies.[34–37] To elucidate fine structures in the DBAR spectra upon field reversal, further study using single crystals is in progress.

The relative amplitude of the differential DBAR spectra of the Fe, Co, and Ni samples seems to coincide with the trend of effective magnetization of these metals. To confirm this, the area intensity of the differential DBAR spectrum was evaluated as $I = \int_{-\infty}^{+\infty} |(N_\uparrow(p) - N_\downarrow(p)|dp$. Table I lists these values and the effective magnetizations. The area intensity of the Fe sample is normalized to 2.2 ($= M_{\mathrm{eff}}$ for Fe). The area intensities of the other samples are normalized to that of the Fe sample. It is found that the area intensities of the Fe and Co samples are in good agreement with the effective magnetizations. That of the Ni sample is a little smaller than that of the effective magnetization. But, the overall trends of the area intensity and the magnetization are similar to each other. The above results indicate that the magnetization of a magnetic substance can be estimated from the magnitude of the field-reversal asymmetry of the DBAR spectrum using a reference sample with known magnetization. Considering the fact that the electron polarization of Fe is at most about 40% near

TABLE I. Area intensities of the differential DBAR spectra (I) for the Fe, Co, and Ni samples and the effective magnetizations (M_{eff}). The unit is μ_B (the Bohr magneton). The area intensity of the Fe sample is normalized to 2.2. The area intensities of the other samples are relative values to that of the Fe sample. The errors are less than 0.1.

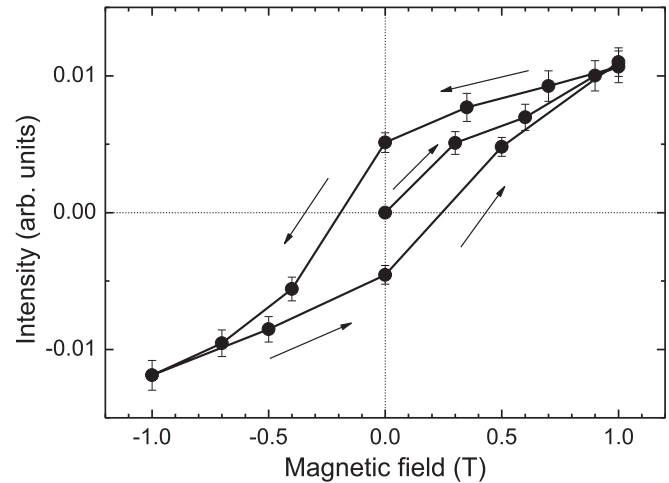|	Fe	Co	Ni
I	2.2	1.8	0.4
M_{eff}	2.2	1.7	0.6

FIG. 3. Area intensities of the differential DBAR spectra between finite and zero magnetic fields as a function of magnetic field. If the differential spectrum exhibits negative and positive amplitudes around the central and tail regions, respectively, as shown in Fig. 2, then the sign of intensity is defined as positive. Conversely, if the differential spectrum exhibits the opposite feature, then the sign is negative.

the Fermi level, the determination of electron polarizations of half-metals by the present method is feasible.[19,21]

The field-reversal asymmetry of the DBAR spectrum for the Gd sample is rather weak even though the effective magnetization of Gd is high ($7\mu_B$). The field-reversal asymmetry depends on the electron and positron polarizations, the overlap of positron and electron wave functions, the internal magnetic field, and the Curie temperature. The annihilation probability between positrons and inner $4f$ shell-shell electrons is generally lower as compared to outer-shell electrons. The Curie temperature of Gd is also low (288 K). Thus, it is not straightforward to determine the magnetization of the Gd sample through a comparison with the $3d$ magnetic substances. To observe much stronger field-reversal asymmetry of Gd, low-temperature experiments might be important.

Figure 3 shows the magnetic field dependence of the area intensity of the differential spectra between finite and zero fields ($= \int_{-\infty}^{+\infty} |N_{B\neq0}(p) - N_{B=0}(p)|dp$) for the Fe sample. Positive intensity means that the differential spectrum exhibits negative and positive intensities around central and tail regions as shown in Fig. 2. Negative intensity corresponds to the opposite case. The differential intensity shows hysteresis that is similar to the magnetization curve. This suggests that the magnetization mechanisms (e.g., ferromagnetism, paramagnetism, roles of spin, and orbital magnetic moments, etc.) can be studied from the field effect on the DBAR spectrum.

In conclusion, we have examined SP-PAS measurements for Fe, Co, Ni, and Gd polycrystals based on the DBAR method with highly polarized positrons. Dependences of the DBAR spectra on magnetic field are related to the magnetic properties of these metals. In SP-PAS experiments, polarized electrons are directly detected through annihilation with polarized positrons. This is an important feature for the investigation of polarized electron states. Development of a spin-polarized positron beam will further enable the study of spin-related phenomena occurring near surfaces and interfaces.

*kawasuso.atsuo@jaea.go.jp

[1] S. S. Hanna and R. S. Preston, Phys. Rev. **106**, 1363 (1957).

[2] P. W. Zitzewitz, J. C. Van House, A. Rich, and D. W. Gidley, Phys. Rev. Lett. **43**, 1281 (1979).

[3] A. Kawasuso and M. Maekawa, Appl. Surf. Sci. **255**, 108 (2008).

[4] P. G. Coleman and A. Kallis, J. Phys.: Conf. Ser. **262**, 012016 (2011).

[5] Y. K. Kato, R. C. Myers, A. C. Gossard, and D. D. Awschalom, Science **306**, 1910 (2004).

[6] C. R. Ast, J. Henk, A. Ernst, L. Moreschini, M. C. Falub, D. Pacile, P. Bruno, K. Kern, and M. Grioni, Phys. Rev. Lett. **98**, 186807 (2007).

[7] D. W. Gidley, A. R. Köymen, and T. W. Capehart, Phys. Rev. Lett. **49**, 1779 (1982).

[8] S. S. Hanna and R. S. Preston, Phys. Rev. **109**, 716 (1958).

[9] P. E. Mijnarends and L. Hambro, Phys. Lett. **10**, 272 (1964).

[10] P. E. Mijnarends, Physica **63**, 248 (1973).

[11] S. Berko and J. Zuckerman, Phys. Rev. Lett. **13**, 339 (1964).

[12] S. Berko, in *Positron Annihilation*, edited by A. T. Stewart and L. O. Roellig (Academic Press, New York, 1967), p. 61.

[13] S. Berko and A. P. Mills, J. Phys. Colloques **32**, C1-287 (1971).

[14] C. Hohenemser, J. M. Weingart, and S. Berko, Phys. Lett. A **28**, 41 (1968).

[15] T. W. Mihalisin and R. D. Parks, Phys. Lett. **21**, 610 (1966).

[16] T. W. Mihalisin and R. D. Parks, Phys. Rev. Lett. **18**, 210 (1967).

[17] T. W. Mihalisin and R. D. Parks, Solid State Commun. **7**, 33 (1969).

[18] N. Shiotani, T. Okada, H. Sekizawa, T. Mizoguchi, and T. Karasawa, J. Phys. Soc. Jpn. **35**, 456 (1973).

[19] M. Šob, S. Szuszkiewicz, and M. Szuszkiewicz, Phys. Status Solidi B **123**, 649 (1984).

[20] T. Jarborg, A. A. Manuel, Y. Mathys, M. Peter, A. K. Singh, and E. Walker, J. Magn. Magn. Mater. **54–57**, 1023 (1986).

[21] S. Szuszkiewicz, M. Šob, and M. Szuszkiewicz, J. Magn. Magn. Mater. **62**, 202 (1986).

[22] P. Genoud, A. K. Singh, A. A. Manuel, T. Jarlborg, E. Walker, M. Peter, and M. Welle, J. Phys. F **18**, 1933 (1988).

[23] P. Genoud, A. A. Manuel, E. Walker, and M. Peter, J. Phys.: Condens. Matter **3**, 4201 (1991).

[24] H. Kondo, T. Kubota, H. Nakashima, T. Kawano, and S. Tanigawa, J. Phys.: Condens. Matter **4**, 4595 (1992).

[25] R. S. Preston and S. S. Hanna, Phys. Rev. **110**, 1406 (1958).

[26] L. A. Page, Rev. Mod. Phys. **31**, 759 (1959).

[27] J. Major, in *Positron Beams and Their Applications*, edited by P. Coleman (World Scientific, Singapore, 1999), p. 259.

[28] Y. Nagai, Y. Nagashima, J. Kim, Y. Itoh, and T. Hyodo, Nucl. Instrum. Methods Phys. Res. B **171**, 199 (2000).

[29] E. Boroński and R. M. Nieminen, Phys. Rev. B **34**, 3820 (1986).

[30] X. Gonze *et al.*, Comput. Mater. Sci. **25**, 478 (2002).

[31] A. Kawasuso, M. Maekawa, and K. Betsuyaku, J. Phys.: Conf. Ser. **225**, 012027 (2010).

[32] V. Sundararajan, D. G. Kanhere, and R. M. Singru, J. Phys.: Condens. Matter **3**, 1113 (1991).

[33] P. Genoud and A. K. Singh, J. Phys.: Condens. Matter **1**, 5363 (1989).

[34] N. Sakai and H. Sekizawa, Rev. Rev. B **36**, 2164 (1987).

[35] Y. Tanaka, N. Sakai, Y. Kubo, and H. Kawata, Phys. Rev. Lett. **70**, 1537 (1993).

[36] M. A. Dixon, J. A. Duffy, S. Gardelis, J. E. McCarthy, M. J. Cooper, S. B. Dugdale, T. Jarlborg, and D. N. Timms, J. Phys.: Condens. Matter **10**, 2759 (1998).

[37] Y. Kakutani, Y. Kubo, A. Koizumi, N. Sakai, B. L. Ahuja, and B. K. Sharma, J. Phys. Soc. Jpn. **72**, 599 (2003).